KSÜ Mühendislik Bilimleri Dergisi, 27(4), 2024
Araştırma Makalesi

KSU J Eng Sci, 27(4), 2024
Research Article

Kahramanmaras Sutcu Imam University
Journal of Engineering Sciences

Geliş Tarihi : 20.05.2024
Kabul Tarihi : 04.11.2024

Received Date : 20.05.2024
Accepted Date : 04.11.2024

EFFECT OF MECHANICAL PROPERTIES OF FILLING MATERIAL ON STATIC AND DYNAMIC BEHAVIOR OF MASONRY ARCH BRIDGES

DOLGU MALZEMESİNİN MEKANİK ÖZELLİKLEİİNİN YIĞMA KEMER KÖPRÜLERİN STATİK VE DİNAMİK DAVRANIŞI ÜZERİNDEKİ ETKİLERİ

Ali Ekber SEVER[1]*(ORCID: 0000-0001-5314-5287)*

[1]Isparta University of Applied Sciences, Department of Civil Engineering, Isparta, Türkiye

*Sorumlu Yazar / Corresponding Author: Ali Ekber SEVER, alisever@isparta.edu.tr

ABSTRACT

The present study examined the impacts of the mechanical properties of the filling material on the seismic behaviour of masonry arch bridges (MAB). A bridge model that did not exist was selected to achieve this objective. Using this model, bridge models with different filling material properties were created in the SAP2000 computer program. Modal analysis and linear time history analysis (THA) were conducted on the aforementioned models to ascertain the filling material's influence on the bridge's dynamic behavior. The findings of the modal analysis indicated that an increase in the density of the filling material increased in the period, while an increase in the elasticity modulus led to a decrease in the period. As a result of linear THA, it was determined that as the density of the filling material increases, the displacements and stresses increase, and as the elastic modulus increases, the displacements and stresses decrease. As a result of static analysis, it was determined that as the density of the filling material increases, the displacement and stress values increase, and as the elastic modulus increases, these values decrease.

Keywords: Arch bridge, filling material, masonry, dynamic analysis, static analysis

ÖZET

Bu çalışmada, dolgu malzemesinin mekanik özelliklerinin yığma kemer köprülerin sismik davranışı üzerindeki etkileri incelenmiştir. Bu amaçla mevcut olmayan bir köprü modeli seçilmiş ve bu köprü modeli kullanılarak farklı dolgu malzemesi özelliklerine sahip köprü modelleri SAP2000 bilgisayar programında oluşturulmuştur. Dolgu malzemesinin köprünün dinamik davranışı üzerindeki etkilerini görebilmek amacıyla bu modeller üzerinde zaman tanım alanında doğrusal analiz ve modal analizler yapılmıştır. Modal analiz sonucunda, kullanılan dolgu malzemesinin yoğunluğu arttıkça periyodun büyüdüğü, elastisite modülü arttıkça ise periyodun küçüldüğü tespit edilmiştir. Zaman tanım alanında yapılan doğrusal analizler sonucunda ise; dolgu malzemesinin yoğunluğu arttıkça yer değiştirme ve gerilmelerin büyüdüğü, elastisite modülü arttığında ise yer değiştirme ve gerilmelerin küçüldüğü tespit edilmiştir. Statik analizler sonucunda, dolgu malzemesinin yoğunluğu arttıkça yer değiştirme ve gerilme değerlerinin arttığı, elastisite modülü arttıkça ise bu değerlerin küçüldüğü tespit edilmiştir.

Anahtar Kelimeler: Kemer köprü, dolgu malzemesi, yığma, dinamik analiz, statik analiz

ToCite: SEVER, AE., (2024). EFFECT OF MECHANICAL PROPERTIES OF FILLING MATERIAL ON STATIC AND DYNAMIC BEHAVIOR OF MASONRY ARCH BRIDGES. *Kahramanmaraş Sütçü İmam Üniversitesi Mühendislik Bilimleri Dergisi*, 27(4), 1248-1266.

INTRODUCTION

An important component of transportation in many places around the world, masonry arch bridge (MAB) represents a priceless part of the cultural and architectural heritage of humanity. MAB has often been damaged or destroyed by unforeseen incidents such as earthquakes. Natural hazards such as earthquakes and floods can significantly damage or destroy such buildings. Consequently, the analysis of the seismic behavior of these bridges through the use of computer modelling is of significant importance for the continued viability of these structures. Many studies have been conducted in the past investigating the dynamic performance of MAB.

Kader et al. (2021) researched the seismic behavior of an MAB using varied damping ratios. They modeled the bridge in the SAP 2000 computer program and analyzed the behavior of the bridge with earthquake acceleration records. They evaluated the stress and displacements obtained as a result of this study. Brencich & Sabia (2008) examined the Tanaro bridge. This bridge, which is an MAB, first applied various tests to obtain the mode shapes and natural frequencies of the MAB and then used these data to construct the numerical model of the bridge. They then analyzed this model at different stages of the bridge's service life and demolition. Sakcali et al. (2019) examined the Irgandı Bridge in Bursa. They created a finite element model of this bridge, which is an MAB, and performed modal and linear dynamic analysis under different earthquake acceleration records. As a result of this study, they stated that maximum displacements occur in the upper part of the bridge and the greatest principal stresses occur in the support region.

Çubuk et al. (2022), in their study, researched the seismic performance of Murat Bey Bridge. They created a model of the MAB in the SAP2000 software and applied modal and time history analyzes (THA) to this model. The results of the aforementioned study revealed the highest stress and displacement values in the bridge. Laterza et al. (2017) researched the dynamic behavior of an MAB in their study. They created a numerical model of this multi-span bridge and performed a pushover analysis. As a consequence of their analysis, they stated that this bridge provided the displacement values demanded by the capacity spectrum method (ATC-40, 1996). Özmen & Sayın (2018) analyzed the Dutpınar bridge utilizing the acceleration records of a previous earthquake in Türkiye. As a consequence of the analysis of the masonry bridge, they modeled with the finite element method, and the largest and smallest shear stresses and strains were obtained.

Harapin et al. (2013) conducted a dynamic and static analysis of an MAB. In this research, the effects of vertical load, seismic effect, and temperature change were investigated. As a result, they stated that the deformation and crack regions obtained from the model they created in the computer program were compatible with the real model. Kumbasaroglu et al. (2019), performed a study to evaluate the seismic performance of an MAB. To this end, they modeled the masonry bridge and made analyzes under the bridge's own weight and earthquake acceleration records from the past. They evaluated the stress and displacement values obtained as a result of their analysis.

Saygılı & Lemos (2021) analyzed the seismic behavior of two historical MABs with different spans and geometries in Türkiye. To achieve this objective, finite and discrete element models of the aforementioned bridges were created in computer programs. Subsequently, time-history analyses were conducted on the aforementioned models. The analysis yielded two key findings. Firstly, the short-span bridge exhibited greater resistance to earthquakes. Secondly, discrete element models were deemed an appropriate tool for the safety evaluation of masonry bridges.

Sözen & Doğangün (2023) conducted a study investigating the seismic performance of an existing historical MAB. For this purpose, they modeled the original and modified versions of this bridge, whose shape changed over time, in a computer program. They evaluated the stress, deformation, and cracks obtained as a result of nonlinear static and dynamic analyses they performed on these models. As a result, they stated that the bridge became more vulnerable to earthquake loads as its shape changed.

In a study conducted by Evci et al. (2024), the seismic behaviour of a historical bridge was examined. To this end, a finite element model of the historical bridge was created in a computer program. A nonlinear THA was performed on the aforementioned model. As a consequence of their analysis, they evaluated the displacements and stresses occurring on the bridge.

There are many studies in the literature investigating the static behavior of masonry arch bridges. In a study conducted by Altunisik et al. (2015), the effects of restoration on the structural behaviour of MAB were investigated. To this

end, the researchers created computer models of both the unrestored and restored versions of an existing bridge. Subsequently, an analysis was conducted on the aforementioned models, evaluating their performance under dead load, live load, and dynamic loads. The displacement and stress results obtained from the aforementioned analyses were then compared. The findings of the study indicate that the restoration process is a crucial factor in the long-term viability of MAB.

Sözen & Çavuş. (2020) researched the behavior of an MAB under seismic loads. In this study, the altered and original forms of the masonry bridge were modeled in the ANSYS computer program. By performing static analysis and THA on these models, deformations and stresses were examined. As a result, they stated that the stiffness increased with the change in the bridge form.

Altunışık et al. (2015), analyzed the behavior of a historical arch bridge under dead and live loads in order to see how the arch thickness affects the structural performance of the bridge. As a result of this study, they revealed that the thickness of the arch affects the structural performance of the bridge.

Although there are many studies in the literature investigating the static and dynamic behavior of MAB, there is no study investigating the effects of the mechanical properties of the infill material on the static and dynamic behavior of MAB. Existing research often emphasizes general factors affecting bridge performance or other material properties, yet the distinct impact of variations in infill material mechanics on structural response has not been fully explored. Therefore, this study aims to address this gap by investigating how different mechanical properties of infill materials affect the overall performance of MAB under both static and dynamic loading conditions.

In this paper, the effects of the mechanical properties of the filling material on the dynamic behavior of masonry arch bridges were investigated. A non-existent bridge model was selected to develop a general understanding of the dynamic behavior of existing masonry arch bridges in Turkey. For this purpose, 9 MABs with different filling material properties were modeled in the SAP2000 computer program. By performing linear THA and modal analysis on these models, the impacts of the mechanical properties of filling material on the seismic performance of MAB were evaluated. In THA analyses, the acceleration record of the Pazarcık earthquake that occurred in Türkiye on February 6, 2023, was used.

CREATING THE FINITE ELEMENT MODEL OF THE BRIDGE

When the studies in the literature are examined, it has been determined that the elasticity modules of the filling materials used in MAB generally vary between 400 - 1500 MPa, and their unit volume weights vary between 13 - 20 kN/m^3 (Özmen & Sayın 2018, Saygılı & Lemos 2021, Onat & Sayın 2015, Bayraktar et al. 2007, Karaton et al. 2017, Pela et al. 2009, Pela et al. 2013, Zampieri et al. 2015, Frunzio et al. 2001). Poisson's ratios are generally taken as 0.2. In this study, in order to see the effects of the mechanical properties of the filling material on the dynamic behavior of masonry arch bridges, three different values are given to the elasticity module and unit weight within the ranges in the literature. The Poisson's ratio is chosen as 0.2. For this reason, 9 bridge models were created by giving different values to the elasticity modulus and density of the filling material. The same material properties of the arch and spandrel wall were used in all bridge models (Özmen & Sayın 2018). The elastic modulus, density, and Poisson's ratio of the arch are 2800 MPa, 28 kN/m^{3,} and 0.2, respectively. The elasticity modulus, density, and Poisson's ratio of the spandrel wall are 2400 MPa, 24 kN/m^{3,} and 0.2, respectively.

In this study, a bridge model that does not exist was chosen to see the effects of the mechanical properties of the filling material on the dynamic behavior of the masonry arch bridges. The reason for choosing a non-existent model is that it provides the opportunity to examine in more detail and freely how the structural and geometric properties of the bridges interact with the mechanical properties of the filling material. This bridge has a length of 28 m, a width of 4 m, and a height of 11.05 m. The spandrel wall of the bridge is 0.5 m thick. These properties were determined by considering the average geometric properties of single-span masonry arch bridges frequently encountered in Turkey. The model created in this way provides a more comprehensive perspective on the seismic performance of existing single-span masonry bridges. The geometric properties of the created models are shown in Figure 1. Fixed supports are assumed on the surfaces of the bridge that are in contact with the ground. It is assumed that there is full adhesion between the elements forming the bridge (arch, spandrel wall, and filling material). The properties of the filling materials are shown in Table 1.

Table 1. Mechanical Properties of Filling Materials

Model Name	Elasticity Modulus of the Filling Material (N/mm^2)	Density of the Filling Material (kN/m^3)	Poisson's Ratio
F1	500	13	0.2
F2	500	16.5	0.2
F3	500	20	0.2
F4	1000	13	0.2
F5	1000	16.5	0.2
F6	1000	20	0.2
F7	1500	13	0.2
F8	1500	16.5	0.2
F9	1500	20	0.2

Three distinct modelling methodologies, namely simplified micro, detailed micro, and macro modelling, are commonly employed for the numerical representation of masonry structures, contingent upon the desired level of precision and the scale of the structural system (Lourenco, 1996). In micro-modelling, which involves the detailed examination of material properties, it is possible to evaluate these separately for mortar and masonry parts. In simplified micro modelling, the masonry parts are widened by half the thickness of the mortar layer, thus ignoring the mortar and segregating the masonry parts from each other by interface lines. In macro modeling, masonry is considered composite without unit and mortar separation. In the study of large building systems, the macro modeling technique is often used, as it greatly shortens the solution time. The macro modeling technique was used in this study. In the macro modeling method, the relationship between the mortar and the masonry unit is neglected. The material is considered as composite (Özmen & Sayın, 2020). Figure 2 shows these modeling methods. The bridge is modeled using Solid element.

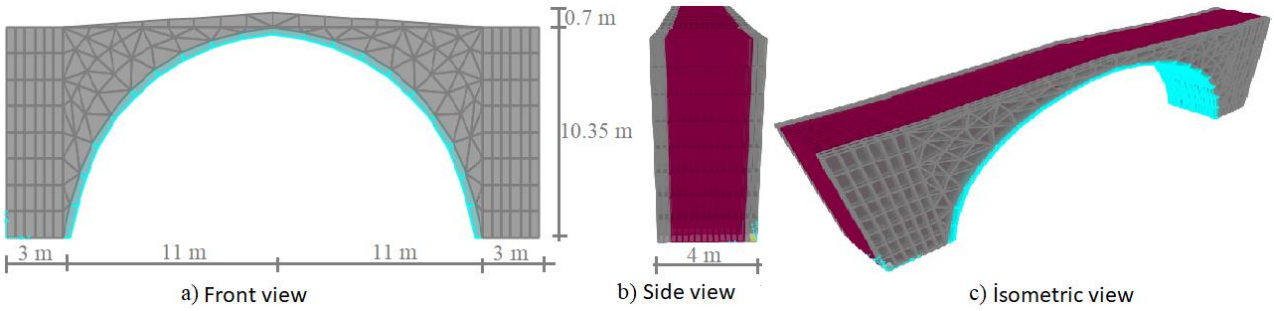

Figure 1. Geometric Properties of The Bridge Model.

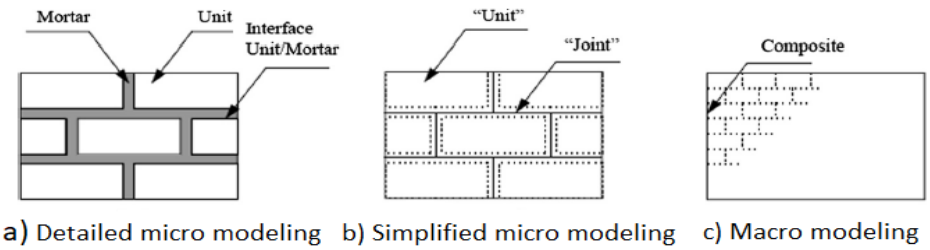

Figure 2. Modeling Methods Used for Masonry Structures (Lourenco 1996).

DETERMİNATİON OF SEİSMİC PARAMETERS

To determine the dynamic behavior of the MAB, acceleration records of a previous earthquake in Türkiye were used. It is assumed that the masonry bridge is located in the center of Isparta and accordingly, earthquake data for the DD-2 earthquake ground motion level defined in the Turkish Building Earthquake Code 2018 (TBDY 2018) were obtained from the Türkiye Earthquake Hazard Map interactive web application (AFAD). Obtained earthquake data are shown in Table 2. Table 3 contains the information about the earthquake used in the seismic analysis. The Seismo Match software was employed to facilitate the matching process for the region in proximity to the arch bridge. The original and matched response spectra obtained from the Seismo Match program are shown in Figure 3a, and the original and matched acceleration records are shown in Figure 3b. To reduce the analysis time, the 35-45 second interval, during which the acceleration record is at its most intense, was utilized.

Table 2. Earthquake Data (AFAD).

Parameter	Definition	Value
Earthquake Ground Motion Level	Earthquake ground motion level with 10% probability of exceedance in 50 years (recurrence period 475 years)	DD2
Ground Class	Medium firm to firm layers of sand, gravel or very solid clay	ZD
S_s	Short period map spectral acceleration coefficient	0.741
S_1	Map spectral acceleration coefficient for a 1.0 second period	0.171

Table 3. The Earthquake Used in The Analysis (AFAD).

Earthquake	Component	Station	M_w	Original		Matched	
				PGA (g)	PGV (cm/s)	PGA (g)	PGV (cm/s)
6 February 2023 Pazarcık	East-West	Pazarcık	7.7	0.567	131.17	0.482	84.00

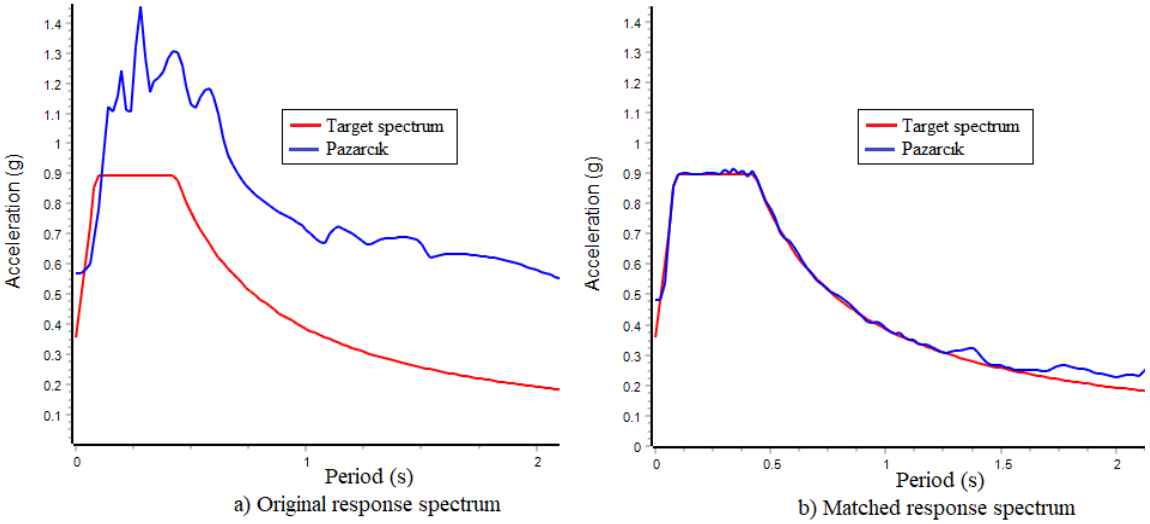

a) Response Spectra

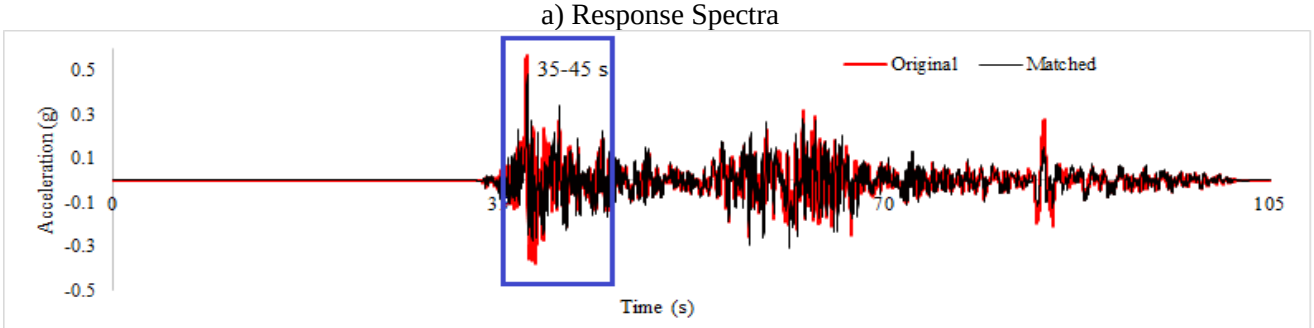

b) Acceleration records

Figure 3. Original and Matched Acceleration Records and Response Spectra (Seismo Match)

ANALYSES

Modal Analysis

Mode shapes play a significant role in the dynamic behavior of arch bridges. Modal analyses were performed on the bridge models in order to obtain the mode shapes and period values of the masonry arch bridge. The damping ratio was chosen as 5% for the modal analysis. While performing modal analysis, solutions were made for 50 modes.

Time History Analysis

A series of linear THA were conducted on the models generated in the SAP2000 program, utilizing the material properties detailed in Table 1. As illustrated in Table 4, the mass participation rates of the first modes are the highest in the y direction in all models. Consequently, THA was conducted exclusively in the y direction (width direction). For the linear THA, the acceleration record of the earthquake, as presented in Table 4, was utilized.

Static Analysis

In this study, a static analysis of the bridge under its own dead load was carried out to see the effects of the mechanical properties of the filling material on the static behavior of the arch bridge.

RESULTS AND DISCUSSION

Results of Modal Analysis

The first six mode shapes and period values derived from the modal analysis are presented in Figure 4. As a result of the modal analysis, the mode shapes obtained from all models are similar to each other. For this reason, only the mode shapes of the F1 model are shown in Figure 4. The mass participation ratios obtained for the 1st and 50th modes as a consequence of the modal analysis are shown in Table 4.

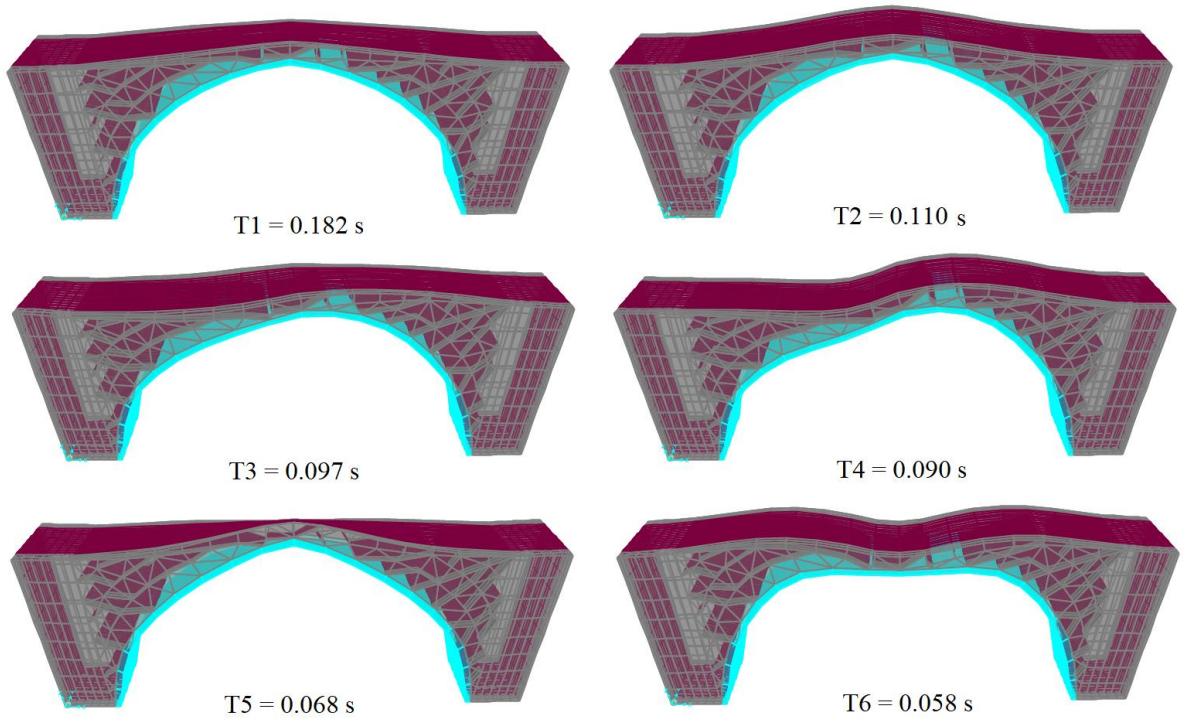

Figure 4. Mode Shapes and Period Values of The F1 Model.

Table 4. Mass Participation Ratios of Masonry Arch Bridge

Model	Mode	Mass participation ratios		
		X direction	Y direction	Z direction
F1	1	3.316E-17	0.41	1.904E-20
	50	0.84104	0.93	0.87887
F2	1	3.525E-17	0.41	1.41E-19
	50	0.85	0.93	0.88
F3	1	3.077E-17	0.40	1.532E-19
	50	0.84758	0.93	0.87792
F4	1	1.338E-17	0.40	1.264E-19
	50	0.83449	0.92	0.8878
F5	1	1.524E-17	0.40	4.455E-20
	50	0.87	0.91	0.89
F6	1	1.447E-17	0.39	2.425E-20
	50	0.87	0.93	0.89
F7	1	8.705E-18	0.39	2.213E-19
	50	0.84	0.91	0.89
F8	1	1.034E-17	0.39	1.941E-19
	50	0.87	0.92	0.89
F9	1	1.058E-17	0.39	2.163E-19
	50	0.87	0.92	0.89

The first period values (T_1) obtained for all models as a consequence of the modal analysis are shown in Figure 5.

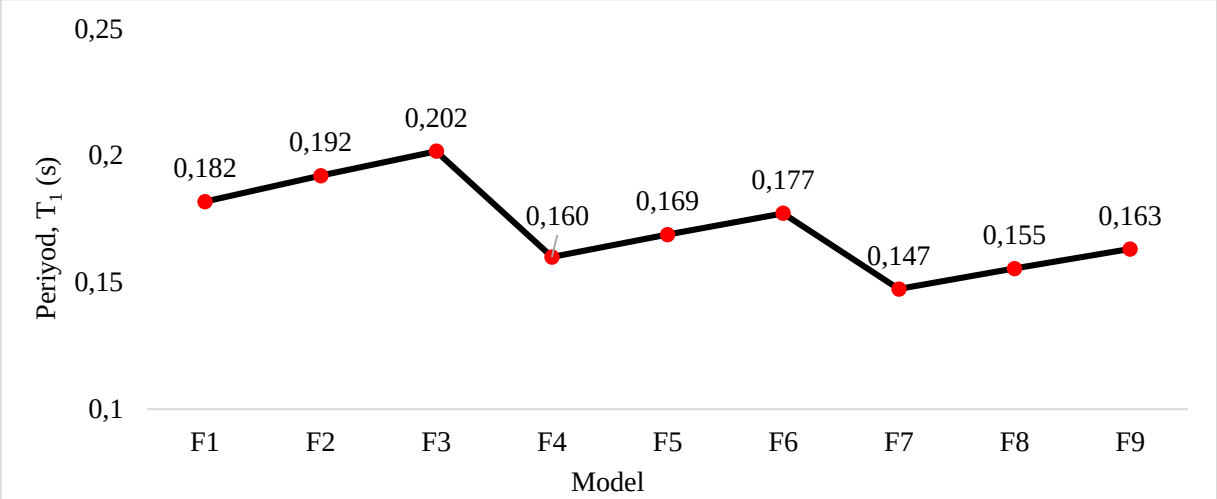

Figure 5. The First Period Values for All Models

As illustrated in Figure 5, the lowest period value was obtained from the F7 model, while the largest period value was obtained from the F3 model. In the F7 model, the filling material exhibited the highest modulus of elasticity and the lowest density, whereas in the F3 model, the filling material exhibited the lowest modulus of elasticity and the highest density. Consequently, the period of the F3 model was 37% larger than that of the F7 model. It can be observed that the period values increase when the elasticity modulus of the filling material is maintained constant and its density is increased. For instance, the period of the F3 model is 11% larger than that of the F1 model. This is a predictable outcome, given that it is well-established that the period value increases as the mass of the structure increases. When the density of the filling material is maintained and the elasticity modulus value is altered, it has been demonstrated that the period value declines as the elasticity modulus rises. It is established that the period is inversely proportional to the stiffness. As the elasticity modulus value increases, the reduction in the period is a predictable consequence of the elevated stiffness.

Figure 6 shows the design spectrum and period range of the analyzed models. Upon examination of Figure 5, it becomes evident that the fundamental periods of all models exhibit a range between 0.147 and 0.202 seconds. Consequently, the interval delineated in red within the graph of Figure 6 represents the aforementioned range.

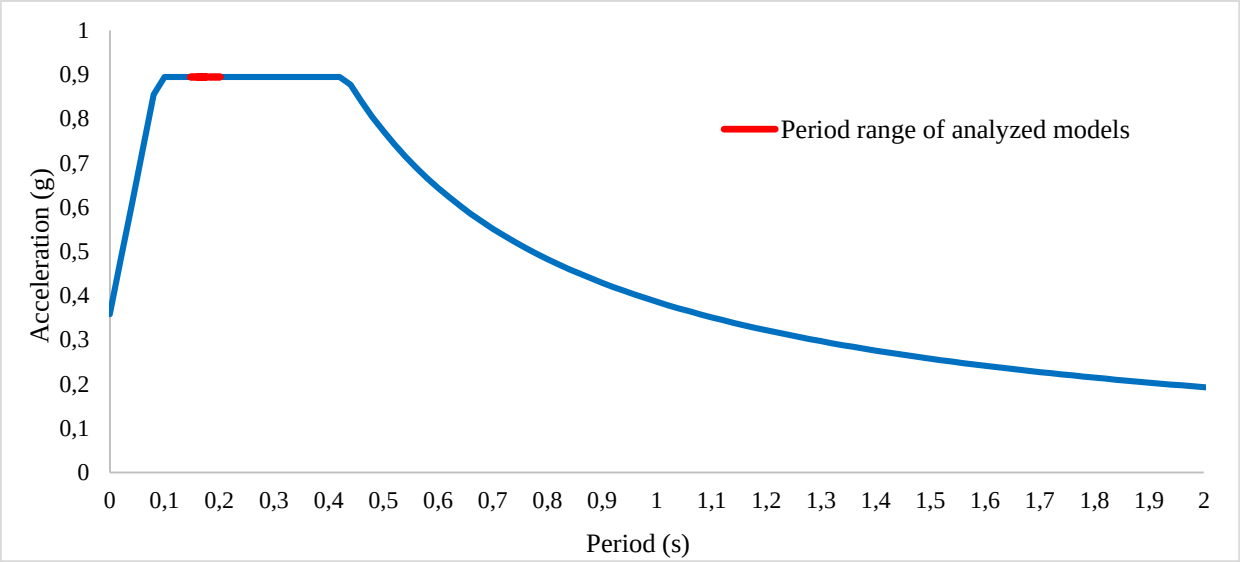

Figure 6. Design Spectrum

Upon examination of Figure 6, it becomes evident that the bridge will be subjected to the greatest acceleration values if its period falls within the range of 0.1-0.44 seconds. The fundamental periods of the analyzed models were found to align with this range. It can be reasonably assumed that if the elasticity modulus of the filling material is increased and its density is reduced, the period will be lower than 0.1 seconds. Consequently, the bridge may be subjected to lower acceleration values.

Results of Time History Analysis

Figure 7 illustrates the base shear forces that occur in all models as a result of THA. Figure 8 illustrates the time-dependent behavior of the base shear forces for the F1, F2, and F3 models. Figure 9 presents a similar analysis for the F2, F5 and F8 models. In the creation of Figures 8 and Figure 9, the 2-6 s interval was utilized, as this was the period during which the highest responses were observed.

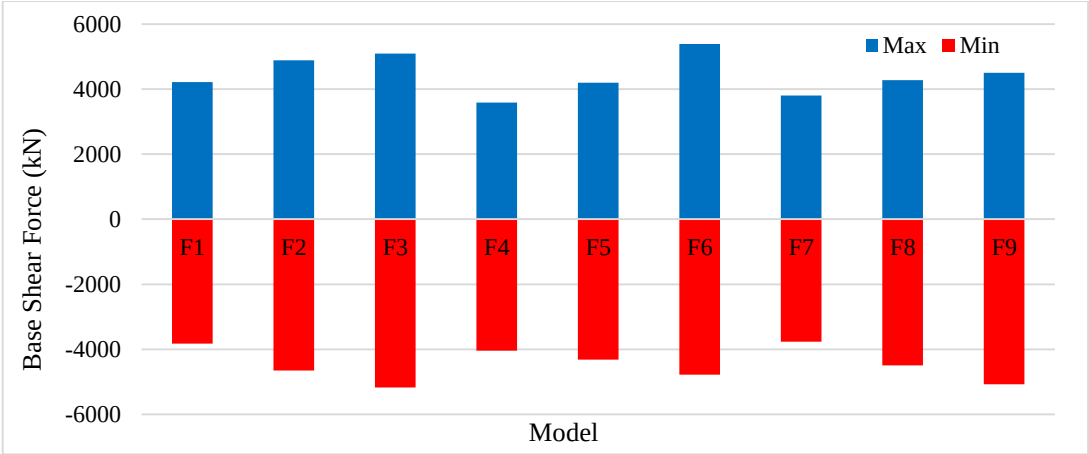

Figure 7. Maximum and Minimum Base Shear Forces

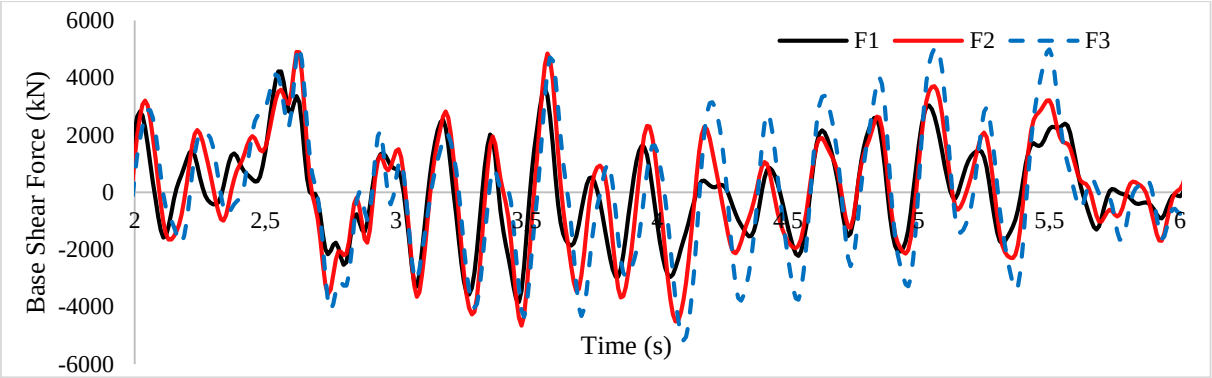

Figure 8. Base Shear Force-Time Graph for F1, F2, And F3 Models

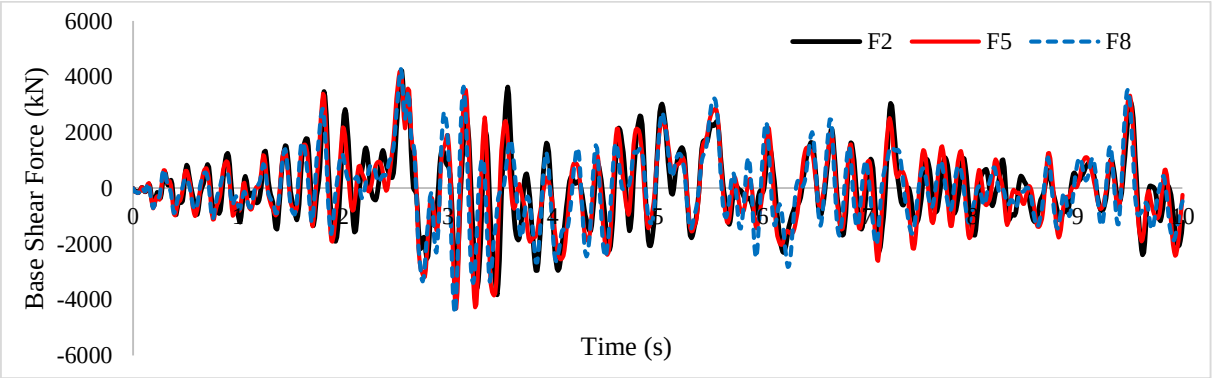

Figure 9. Base Shear Force-Time Graph for F2, F5, And F8 Models

Upon examination of Figures 7 and 8, it becomes evident that the base shear force exhibits a direct correlation with the density of the filling material. For example, the base shear force in the F3 model is 22% higher than that in the F1 model. Upon examination of Figure 9, it is evident that there is no discernible change in the base shear force as a result of the change in the elasticity modulus of the filling material.

A time-history analysis revealed that the highest displacement values were observed at the top of the bridge in all models. Similar results have been obtained in studies conducted in the literature (Sözen & Çavuş 2020, Altunisik et al. 2015, Usta et al 2024, Evci et al 2024, Sevim et al 2011, Saygılı & Lemos 2021). Figures 10 and 11 illustrate the time-dependent displacement of the peak over the 2-6 s interval. Table 5 presents the largest peak displacements and largest stress values observed in all models.

As illustrated in Figure 10, Figure 11, and Table 5, the lowest displacement value was observed in the F7 model, while the highest displacement value was observed in the F3 model. The largest displacement value observed in the F7 model is 44.4% less than that observed in the F3 model. As the density of the filling material increased, the displacement values exhibited a corresponding increase. For example, when comparing the F1 and F3 models, the increase was 24.6%. This result is to be expected, given that greater forces will act on the structure as the density of the filling material increases. As the elastic modulus of the filling material increased, the displacement values exhibited a pronounced decline. For example, when comparing the F2 and F8 models, this reduction was 42.3%. As the elasticity modulus increases, it is to be expected that the displacements will decrease, as the structure becomes more rigid. Consequently, this outcome is also to be expected.

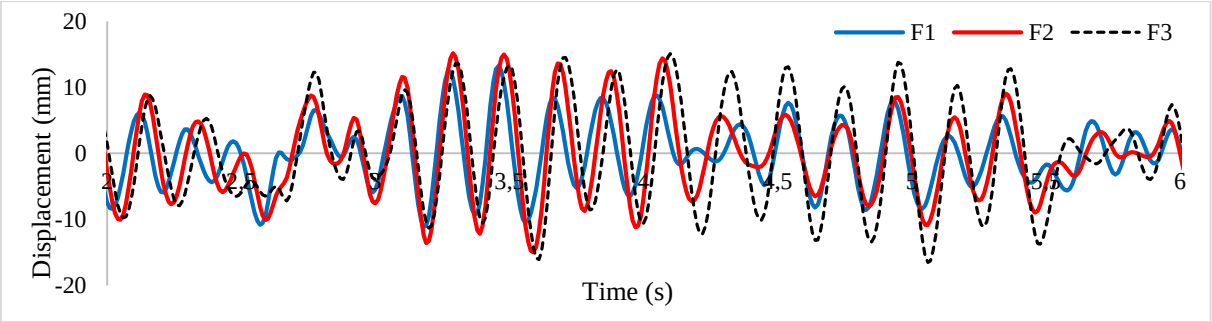

Figure 10. Displacement – Time Graph for F1, F2 And F3 Models

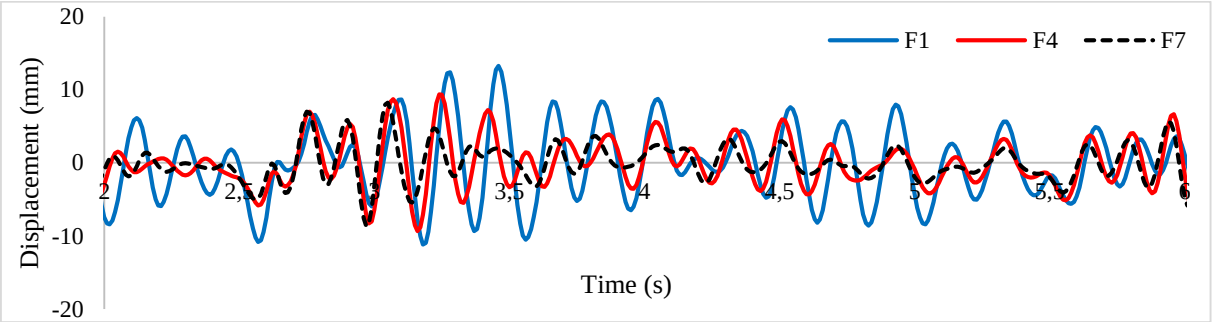

Figure 11. Displacement – Time Graph for F1, F4 And F7 Models

Table 5. Max displacement and stress values.

Model	F1	F2	F3	F4	F5	F6	F7	F8	F9
Max Displacement (mm)	13.26	15.16	16.52	9.38	11.92	12.71	8.69	8.75	10.54
Normal Stress (MPa)	1.271	1.459	1.563	1.075	1.346	1.426	1.005	1.085	1.277
Shear Stress (MPa)	0.316	0.360	0.393	0.23	0.292	0.316	0.224	0.225	0.263
Smax Stress (MPa)	1.277	1.494	1.594	1.081	1.354	1.433	1.001	1.063	1.284
Smin Stress (MPa)	1.277	1.494	1.594	1.081	1.354	1.433	1.001	1.063	1.284

Upon examination of Table 5, it becomes evident that the model exhibiting the lowest levels of stress is F7, while the model exhibiting the highest levels of stress is F3. For instance, when the stresses observed in these two models are contrasted, the largest normal stress, shear stress, and maximum/minimum principal stress values obtained from the F3 model are, respectively, 55.5%, 75.5%, and 59.2% greater than those observed in the F7 model. As the density of the filling material increased, the maximum values of normal stress, shear stress, and maximum/minimum principal stress also increased. As the elastic modulus of the filling material increased, the maximum value of normal stress, shear stress, and maximum/minimum principal stress decreased.

Figure 12, Figure 13, Figure 14, and Figure 15 illustrate the stress, shear stress, maximum principal stress, and minimum principal stress contours that were generated in the F1 model as a consequence of the THA. The contours in these figures were obtained from the 3.46th second of the earthquake. As the stress contours are similar in all models, only the contours of the F1 model are shown. As illustrated in Figure 12, the maximum normal stress values were observed at the top of the arch and the top of the bridge sides. Similar results were obtained in studies conducted in the literature (Altunisik, 2015, Saygılı & Lemos 2021, Bayraktar & Hökelekli 2021, Evci et al 2024). As illustrated in Figure 13, the highest values of shear stresses were observed in the central regions of the arch.

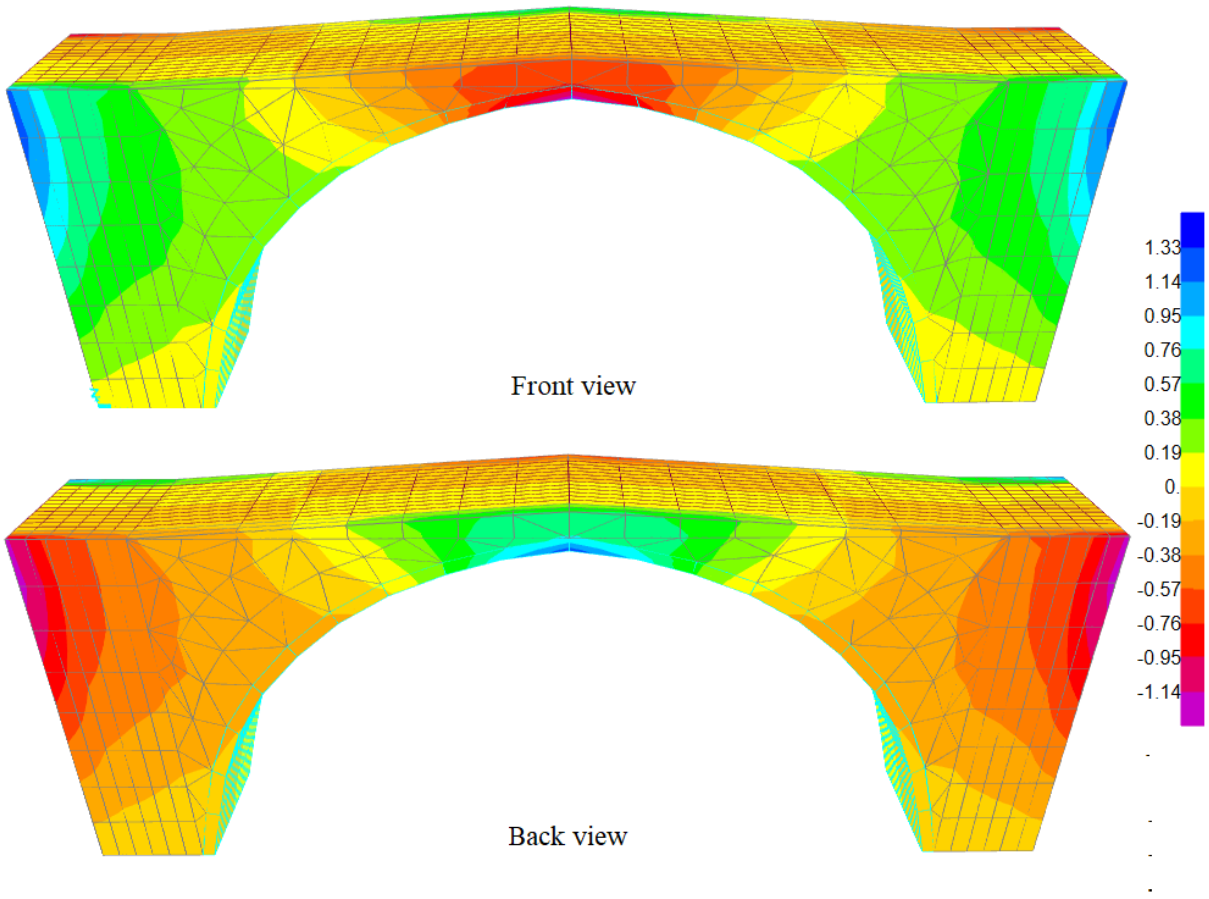

Figure 12. Normal Stress Contour for F1 Model (MPa).

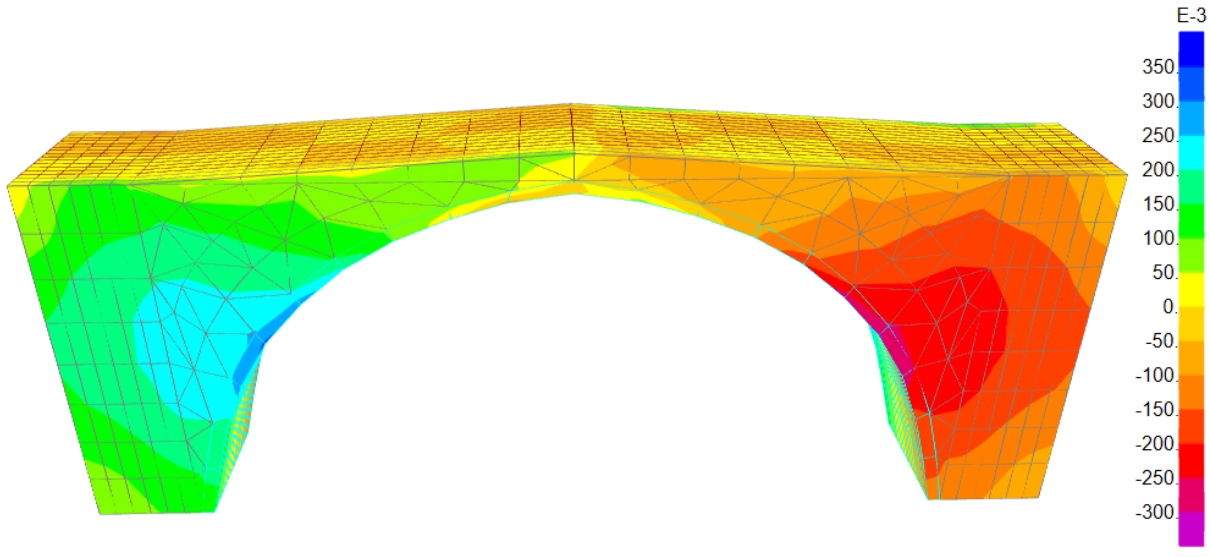

Figure 13. Shear Stress Contour for F1 Model (MPa).

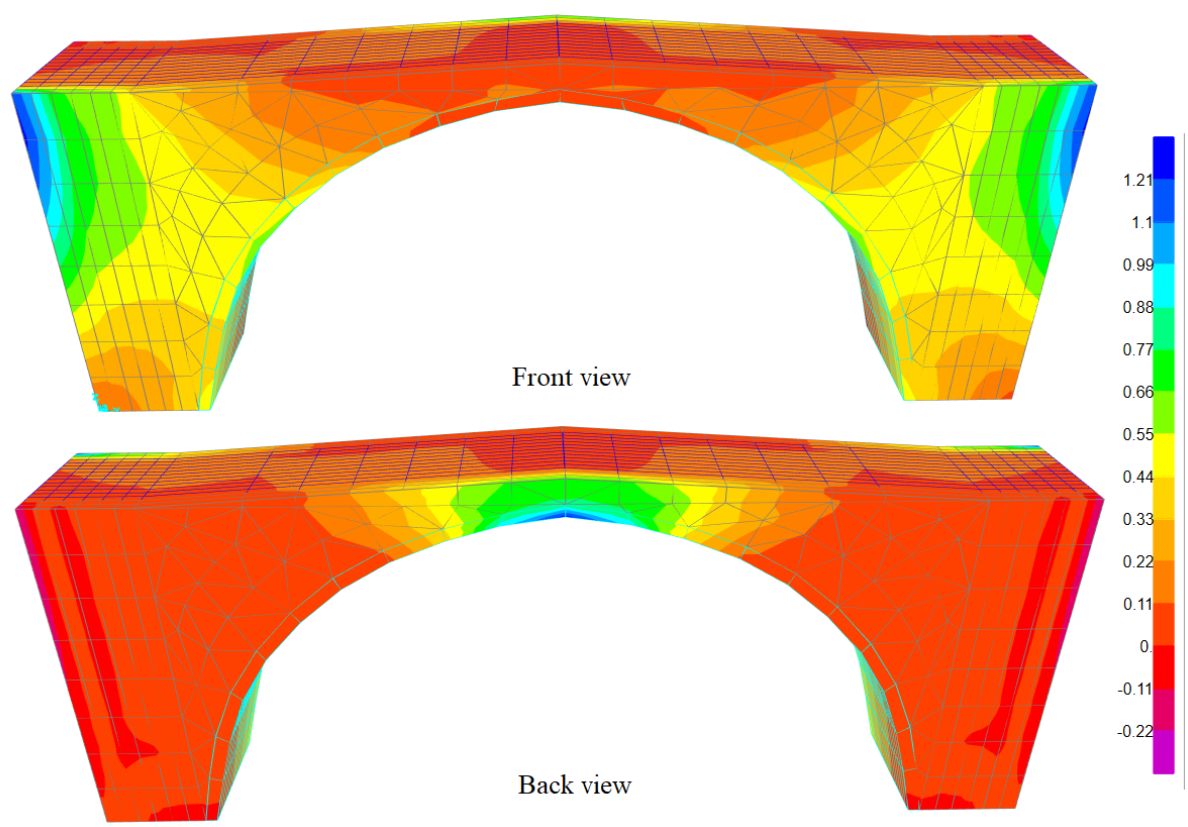

Figure 14. Smax Contour for F1 Model (MPa)

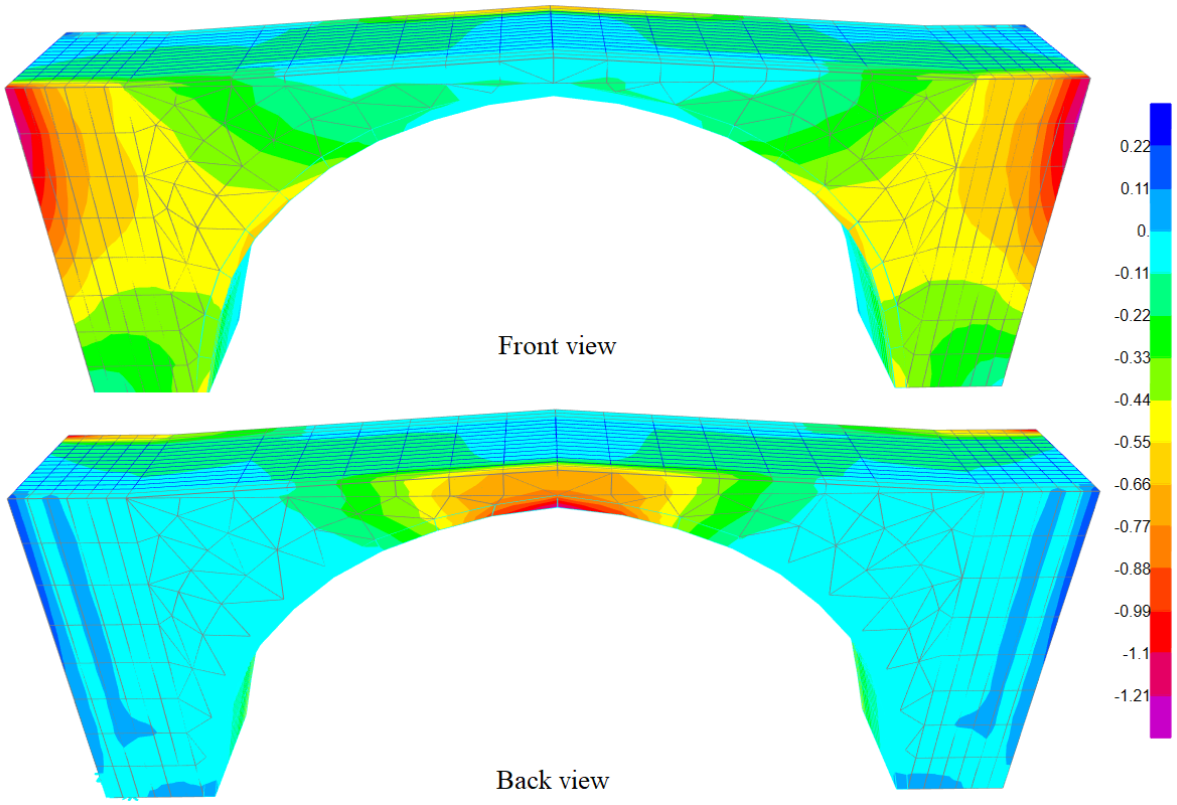

Figure 15. Smin Contour for F1 Model (MPa)

Upon examination of Figures 14 and 15, it becomes evident that the maximum and minimum principal stresses are concentrated at the top of the arch and on the sides of the bridge. A review of studies in the literature investigating the seismic performance of masonry arch bridges using nonlinear methods showed that there were studies that

expected damage to occur at the top of the arch or the sides of the bridge. (Sakcalı et al 2019, Özmen & Sayın 2023, Karaton et al. 2017). Figures 16, 17, 18, and 19 illustrate the maximum and minimum principal stress for the range of 2-6 s, as a function of time. Upon examination of Figures 16 and 18, it becomes evident that the maximum and minimum principal stresses occurring in the bridge undergo a transformation as the density of the filling material increases over time. The aforementioned graphs demonstrate that the utilization of high-density filling material will result in the exposure of greater maximum and minimum principal stresses during an earthquake. Figures 17 and 18 illustrate the effect of an increase in the elasticity modulus on the same graph. Upon examination of these figures, it can be observed that the utilization of a filling material with a high modulus of elasticity will result in a reduction in the maximum and minimum principal stresses experienced by the bridge during an earthquake.

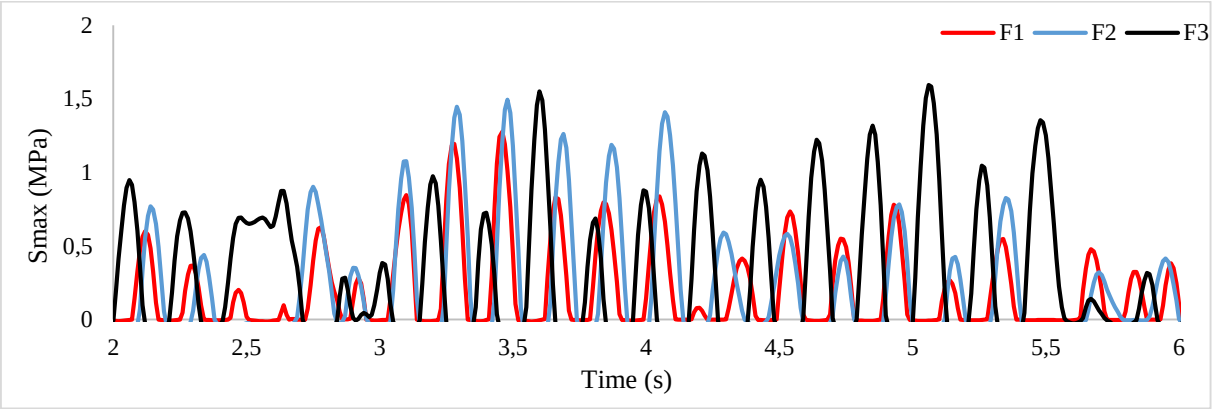

Figure 16. Maximum Principal Stress-Time Diagram for Models F1, F2, and F3

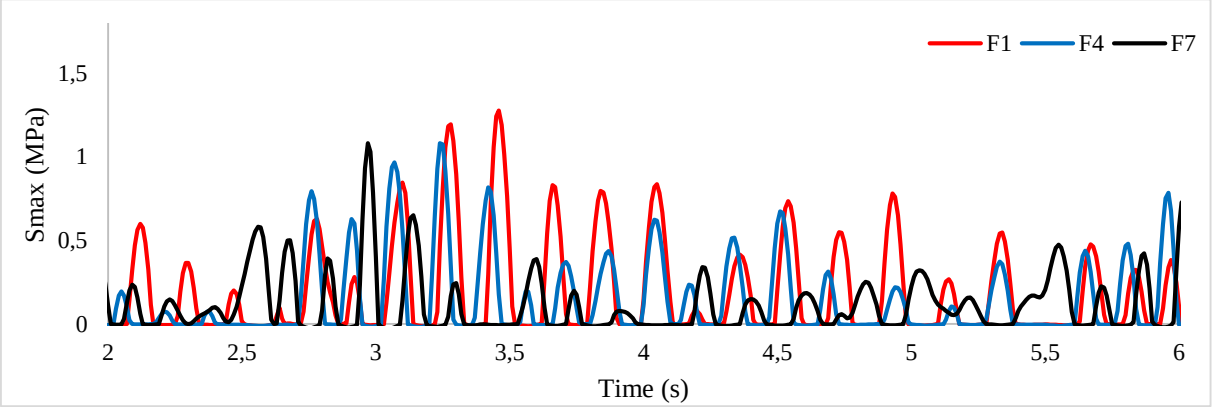

Figure 17. Maximum Principal Stress-Time Diagram for Models F1, F4, and F7

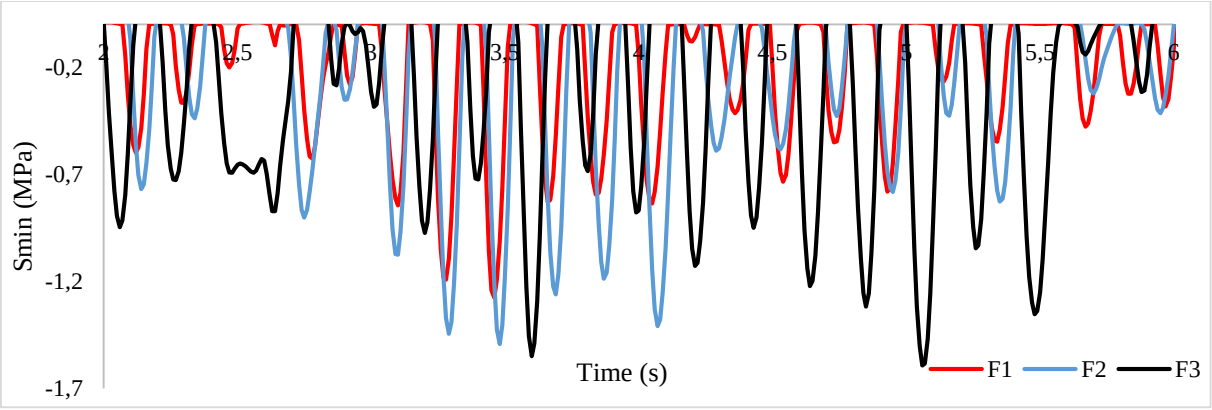

Figure 18. Minimum Principal Stress - Time Diagram for Models F1, F2, and F3

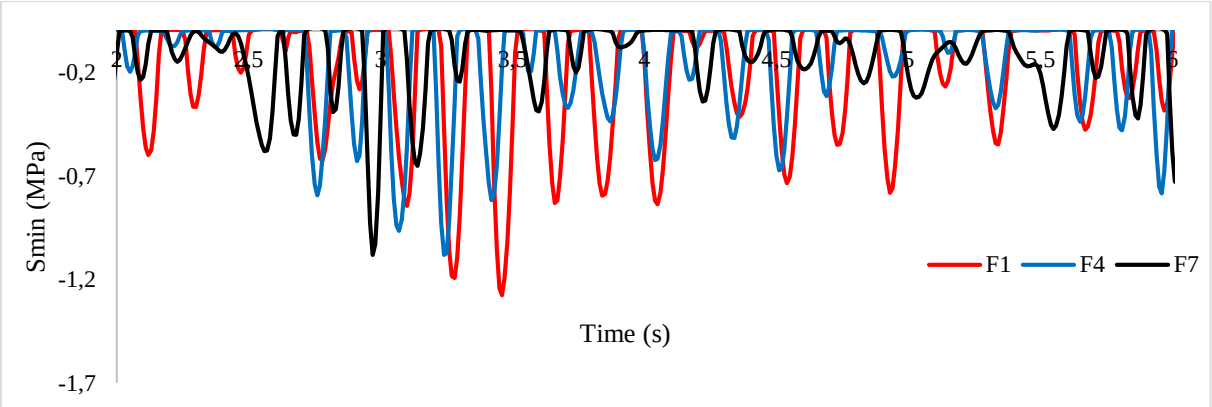

Figure 19. Minimum Principal Stress - Time Diagram for Models F1, F4, and F7

Results of Static Analysis

The largest vertical displacements resulting from the static analysis of the models are illustrated in Figure 20.

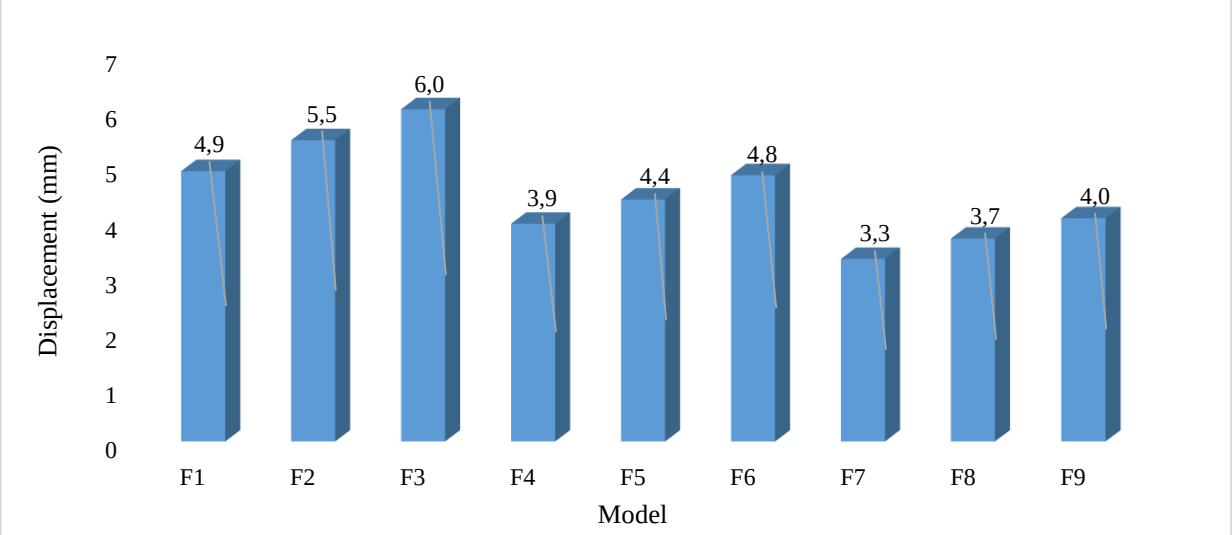

Figure 20. Vertical Displacement Graph

As seen in Figure 20, the largest displacement increases with increasing infill density. For example, the vertical displacement in the F3 model is 22.4% greater than in the F1 model. As the modulus of elasticity increased, the largest vertical displacement decreased. For example, the displacement in the F7 model is 32.7% less than in the F1 model. The largest vertical displacement occurs in model F3, while the smallest displacement occurs in model F7. The displacement value obtained from model F3 is 82% greater than the displacement value obtained from model F7. These results show that the mechanical properties of the infill material have a great influence on the static behavior of the masonry arch bridge.

Figure 21 illustrates the vertical displacement contour observed in the F1 model as a consequence of the static analysis. As identical displacement contours are observed in all models, only the contour of the F1 model is presented herewith. As can be seen in Figure 21, the largest vertical displacements occurred in the middle and upper parts of the bridge. Similar results were obtained in studies conducted in the literature (Sözen & Çavuş, 2020, Altunışık et al. 2015, Nemutlu et al. 2023, Altunisik et al. 2015).

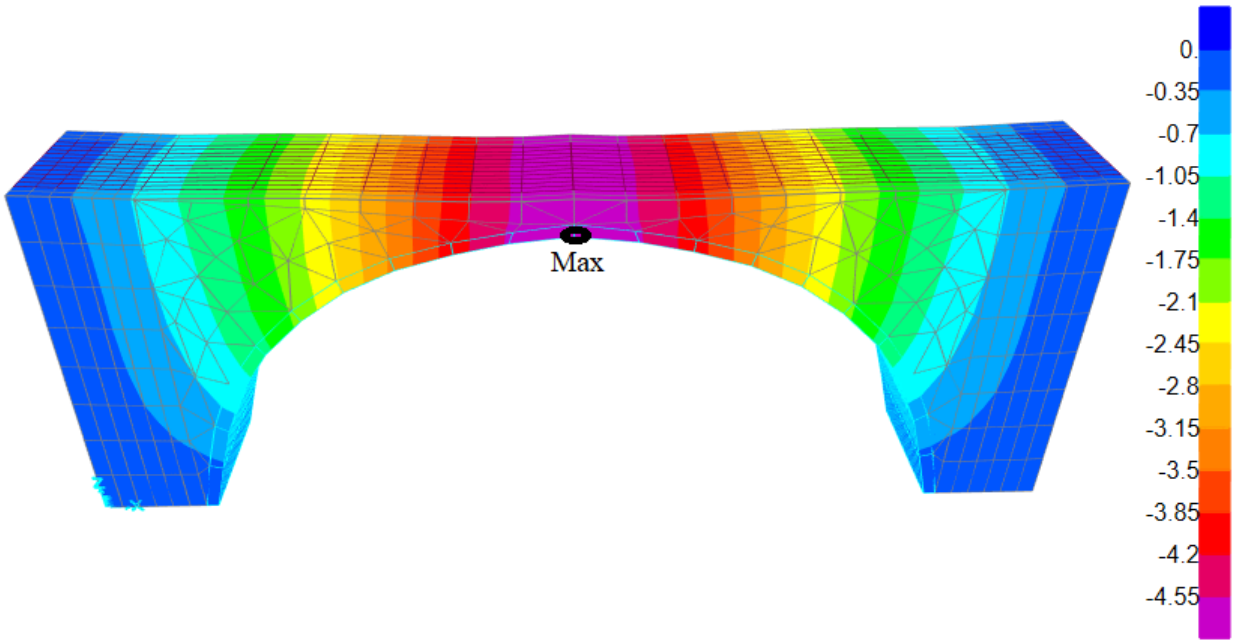

Figure 21. Vertical Displacement Contour of F1 Model (mm)

Figure 22 shows the maximum compressive and tensile stresses that occur in bridge models as a result of static analysis.

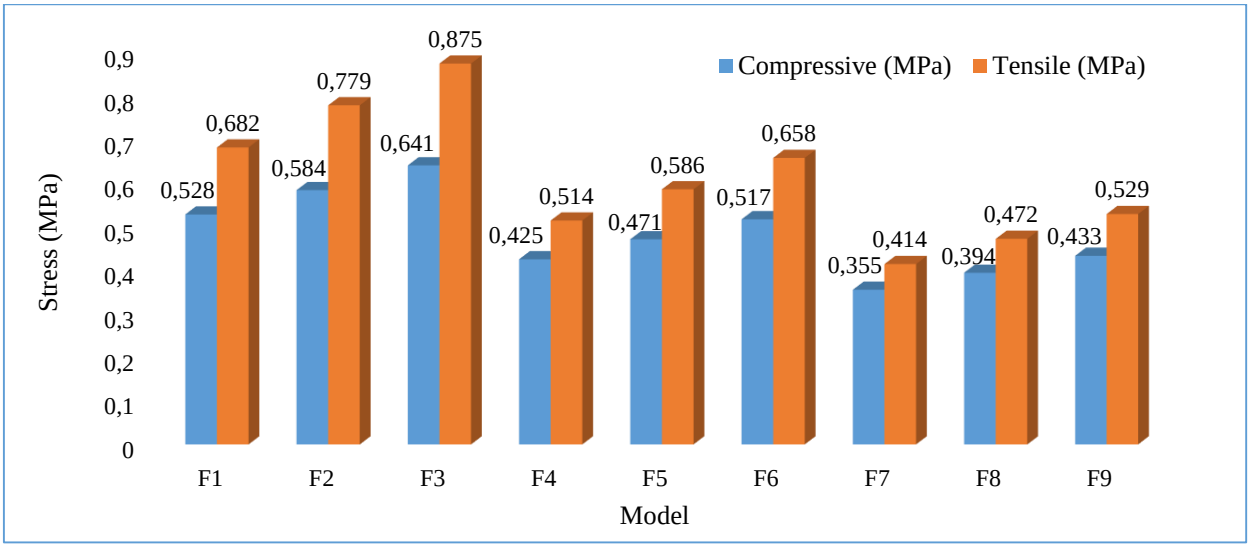

Figure 22. Graph of Compressive and Tensile Stresses

As seen in Figure 22, tensile and compressive stresses increased with the increase in the density of the filling material. For example, the maximum compressive and tensile stresses obtained from model F3 are 21.4% and 28.3% larger than model F1, respectively. As the elasticity modulus of the filling material increased, the compressive and tensile stresses decreased. For example, the compressive and tensile stresses obtained from model F7 are 32.8% and 39.3% smaller, respectively, compared to model F1. The highest compressive and tensile stresses occurred in model F3, while the lowest stresses occurred in model F7. The maximum compressive and tensile stresses in model f3 are 80.6% and 111.4% larger than those in model f7, respectively.

The normal stress contour occurring in the F1 model as a result of the static analysis is shown in Figure 23. As identical normal stress contours are observed in all models, only the contour of the F1 model is presented herewith.

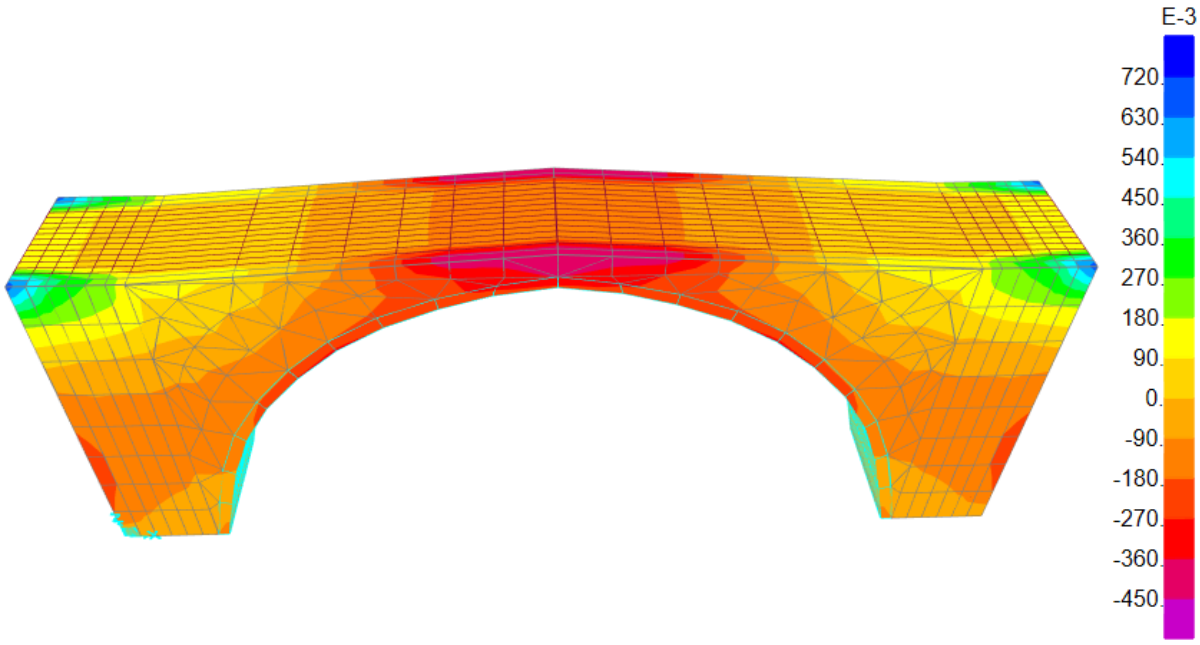

Figure 23. Normal Stress Contour of F1 Model (MPa)

As can be seen in Figure 23, the compressive stresses are concentrated in the upper parts of the arch, while the tensile stresses are concentrated in the upper part of the side supports. Similar results were obtained in studies conducted in the literature (Sözen & Çavuş 2020, Altunışık et al. 2015, Altunisik et al. 2015).

CONCLUSION

The objective of this study was to investigate the effects of the mechanical properties of the filling material used in masonry arch bridges on the static and dynamic behavior of the bridge. To this end, nine bridge models of identical dimensions and exhibiting disparate mechanical properties of the filling material were generated within the SAP2000 program. Static analysis, modal analysis, and THA were conducted to elucidate the behavior of the bridges. The results of the analyses are presented in the following table.

The results of the modal analysis indicated that similar mode shapes were observed in all models. It was observed that the fundamental periods of all models varied between 0.147 s and 0.202 s. It has been demonstrated that as the density of the filling material increases, the period of vibration also increases. Conversely, as the elasticity modulus of the filling material increases, the period of vibration decreases. The model exhibiting the lowest period is the one with the lowest density of the filling material and the highest modulus of elasticity.

The results of the THA indicated that the highest displacement values were observed at the top of the bridge in all models. As the density of the filling material increased, it was found that the base shear force, maximum displacement, normal stress, shear stress, and maximum/minimum principal stresses all increased. For example, the maximum displacement, base shear force, normal, shear, and principal stresses obtained from the F3 model are 25%, 22%, 23%, 24%, and 25% larger than those from the F1 model, respectively. Conversely, as the elasticity modulus of the filling material increased, the opposite occurred. It was observed that while normal stress and maximum/minimum principal stresses were concentrated in the upper parts of the sides of the bridge and the upper part of the arch, shear stresses reached their largest values in the middle parts of the arch. For example, the maximum displacement, base shear force, normal, shear, and principal stresses obtained from the F8 model are 42%, 8%, 26%, 38%, and 28% smaller than those from the F2 model, respectively.

The results of the static analysis demonstrated that as the density of the filling material increased, the values of displacement, compressive stress, and tensile stress also increased. Conversely, an increase in the elasticity modulus of the filling material results in a corresponding decrease in the aforementioned values. The highest values of compressive stress were observed in the upper regions of the arch, while the highest values of tensile stress were observed in the upper regions of the edge supports.

Consequently, it has been demonstrated that the mechanical properties of the filling material employed in the construction of MAB exert a significant influence on the static and dynamic behavior of the bridge. It has been demonstrated that the utilization of filler material with a low density and high modulus of elasticity in the construction of masonry arch bridges represents a superior approach in terms of the static and seismic behavior of the bridge.

REFERENCES

Afet ve Acil Durum Yönetimi Başkanlığı. "Türkiye Bina Deprem Yönetmeliği". Ankara, Türkiye, 2018.

Afet ve Acil Durum Yönetimi Başkanlığı. "Türkiye Deprem Tehlike Haritaları İnteraktif Web Uygulaması" https://tdth.afad.gov.tr/TDTH/main.xhtml (20.03.2023).

Altunışık, A.C., Kanbur, B., Genc, A.F., (2015). The effect of arch geometry on the structural behavior of masonry bridges. *Smart Struct. Syst*, 16(6), 1069-1089. https://doi.org/10.12989/sss.2015.16.6.1069

Altunisik, A. C., Bayraktar, A., & Genc, A. F. (2015). Determination of the restoration effect on the structural behavior of masonry arch bridges. *Smart Struct. Syst, 16*(1), 101-139. http://dx.doi.org/10.12989/sss.2015.16.1.101

ANSYS, 2008. Swanson Analysis System, US.

ATC-40, (1996), Seismic Evaluation and Retrofit of Concrete Buildings-Vol.1, Applied Technology Council, Redwood City, CA

Bayraktar, A., Altunısık, A. C., Türker, T., & Sevim, B. (2007). The effect of finite element model updating on earthquake behaviour of historical bridges. In Sixth National Conference on Earthquake Engineering, Istanbul, Turkey, October (pp. 16-20).

Bayraktar, A., & Hökelekli, E. (2021). Nonlinear soil deformability effects on the seismic damage mechanisms of brick and stone masonry arch bridges. International Journal of Damage Mechanics, 30(3), 431-452. https://doi.org/10.1177/1056789520974423

Brencich, A. and Sabia, D., (2008). Experimental identification of a multi-span masonry bridge: The Tanaro Bridge. *Construction and Building Materials*, 22(10), 2087-2099. https://doi.org/10.1016/j.conbuildmat.2007.07.031

Çubuk E.G., Sayın E., and Özmen, A., (2022). Dynamic Analysis of Historical Masonry Arch Bridges under Different Earthquakes: The Case of Murat Bey Bridge. *Turkish Journal of Science & Technology*, 17(2). https://doi.org/10.55525/tjst.1105998

Evci, P. U., Sever, A. E., & Şakalak, E. (2024). Investigation of Seismic Behavior of the Historical Yeşiltepe Bridge. *Prevention and Treatment of Natural Disasters*, *3*(2). https://doi.org/10.54963/ptnd.v3i2.291

Frunzio, G., Monaco, M., & Gesualdo, A. (2001). 3D FEM analysis of a Roman arch bridge. Historical constructions, 591-598.

Harapin, A., Smilović, M., Grgić, N., Glibić, M., Radnić, J., (2013). Static and dynamic analysis of the old stone bridge in Mostar. *Gradevinar* 64, 655-655. https://doi.org/10.14256/JCE.715.2012

Kader, A., Sayın, E. and Özmen, A., (2021). Farklı Sönüm Tipleri Altında Tarihi Yığma Köprülerin Sismik Tepkilerinin Değerlendirilmesi. *Fırat Üniversitesi Mühendislik Bilimleri Dergisi*, 34(1), 45-59. https://doi.org/10.35234/fumbd.940435

Karaton, M., Aksoy, H. S., Sayın, E., & Calayır, Y. (2017). Nonlinear seismic performance of a 12th century historical masonry bridge under different earthquake levels. Engineering Failure Analysis, 79, 408-421. https://doi.org/10.1016/j.engfailanal.2017.05.017

Kumbasaroglu, A., Celik, A., Demir, O., Turan, A. & Yalciner, H., (2019). An Assessment of the Seismic Performance of the Historic Tigris Bridge. *Open Journal of Civil Engineering*, 9(03), 230. https://doi.org/10.4236/ojce.2019.93016

Laterza, M., D'Amato, M., & Casamassima, V.M., (2017). Seismic performance evaluation of multi-span existing masonry arch bridge. In AIP Conference Proceedings (Vol. 1863, No. 1, p. 450010). AIP Publishing LLC. https://doi.org/10.1063/1.4992619

Lourenco, P.B., (1996). Computational strategy for masonry structures. *Delft University of Technology and DIANA Research*.

Nemutlu, Ö. F., Güzel, İ., Balun, B., Öztürk, M., & Sarı, A. (2023). Nonlinear Seismic Assessment of Historical Masonry Karaz Bridge Under Different Ground Motion Records. *Bitlis Eren Üniversitesi Fen Bilimleri Dergisi*, *12*(1), 247-260. https://doi.org/10.17798/bitlisfen.1232008

Onat, O., & Sayın, E. (2015). Tarihi Tağar Köprüsünün doğrusal olmayan sismik analizi. 5. Tarihi Eserlerin Güçlendirilmesi ve Geleceğe Güvenle Devredilmesi Sempozyumu, 1-3.

Özmen, A. and Sayın, E., (2018). Seismic assessment of a historical masonry arch bridge. *Journal of Structural Engineering & Applied Mechanics*, 1(2), 95-104, 2018. https://doi.org/10.31462/jseam.2018.01095104

Özmen, A. and Sayın, E., (2020). Tarihi yığma bir köprünün deprem davranışının değerlendirilmesi. *Niğde Ömer Halisdemir Üniversitesi Mühendislik Bilimleri Dergisi*, 9(2), 956-965. https://doi.org/10.28948/ngumuh.715121

Özmen, A., & Sayın, E. (2023). 3D soil structure interaction effects on the seismic behavior of single span historical masonry bridge. *Geotechnical and Geological Engineering*, *41*(3), 2023-2041. https://doi.org/10.1007/s10706-023-02389-6

Pela, L., Aprile, A., Benedetti, A., (2009). Seismic assessment of masonry arch bridges. *Engineering Structures*, 31: 1777- 1788. https://doi.org/10.1016/j.engstruct.2009.02.012

Pelà, L., Aprile, A., & Benedetti, A. (2013). Comparison of seismic assessment procedures for masonry arch bridges. Construction and Building Materials, 38, 381-394. https://doi.org/10.1016/j.conbuildmat.2012.08.046

Sakcalı, G.B., Gönül, A. and Yüksel, İ., (2019). Seismic behavior of historical masonry bridges: The case study of Irgandi Bridge. *International Journal*, 6, 25. https://doi.org/10.15377/2409-9821.2019.06.4

SAP2000. Integrated Finite Element Analysis and Design of Structures Basic Analysis Reference Manual. Berkeley, California, Computer and Structres Inc.

Saygılı, Ö., & Lemos, J. V. (2021, October). Seismic vulnerability assessment of masonry arch bridges. In Structures (Vol. 33, pp. 3311-3323). Elsevier. https://doi.org/10.1016/j.istruc.2021.06.057

Seismosoft. (2023). SeismoMatch 2023-A Computer Program for Spectrum Matching of Earthquake Records.

Sözen, Ş., & Doğangün, A. (2023). Evaluation of the effect of change in support conditions on the seismic behavior of a historical masonry bridge. *ACM Journal on Computing and Cultural Heritage*, *16*(4), 1-19. https://doi.org/10.1145/3590957

Sevim, B., Bayraktar, A., Altunişik, A. C., Atamtürktür, S., & Birinci, F. (2011). Assessment of nonlinear seismic performance of a restored historical arch bridge using ambient vibrations. *Nonlinear Dynamics*, *63*, 755-770. https://doi.org/10.1007/s11071-010-9835-y

Sözen, Ş. and Çavuş, M., (2020). Tek açıklıklı tarihi taş köprülerde form değişikliğinin köprünün sismik davranışına etkisinin değerlendirilmesi: Niksar Yılanlı (Leylekli) Köprü Örneği. *Düzce Üniversitesi Bilim ve Teknoloji Dergisi*, 8(1), 48-59. https://doi.org/10.29130/dubited.589223

Usta, P., Sever, A. E., Şakalak, E., & Ünveren, C. (2024). Examination of the Seismic Behavior of The Historical Yeşildere Bridge. *Konya Journal of Engineering Sciences*, *12*(2), 432-450. https://doi.org/10.36306/konjes.1427898

Zampieri, P., Zanini, M. A., & Modena, C. (2015). Simplified seismic assessment of multi-span masonry arch bridges. Bulletin of Earthquake Engineering, 13, 2629-2646. https://doi.org/10.1007/s10518-015-9733-2